Amplification of an external signal in an acousto-optic device with delay

C. J. Marriott and C. Delisle
Département de Physique—Laboratoire de Recherches en Optique et Laser, Faculté des Sciences et de Genie, Université Laval, Sainte-Foy, Québec, Québec, Canada G1K 7P4
(Received 20 May 1988)

When an additive external signal is applied to an acousto-optic bistable device showing the Feigenbaum period-doubling route to chaos, various amplification phenomena are observed. We present these phenomena and show the importance of linearized modal and Floquet analyses in their explanation.

INTRODUCTION

It is well known that in the neighborhoods of dynamical instabilities, systems show effects which are independent of the exact physical or mathematical system being studied, but which, in fact, depend only on the type of instability or bifurcation. The best such example is probably the scaling laws for period-doubling bifurcations as determined by Feigenbaum.[1-5] Another such effect is the presence of noisy precursors to bifurcations in the power spectrum. As the bifurcation is approached the frequencies at which new lines appear after the bifurcation are marked by the presence of noise amplification in their neighborhoods.[6,7] This effect has been studied experimentally and analytically by Jeffries and Wiesenfeld on an electronic system,[6] and in the case of a Hopf bifurcation has been observed in an acoustic-optic bistable device by Vallée.[8]

The same phenomena are predicted to be observed if the stochastic noise is replaced by a periodic signal.[9-12] In the case of a periodic signal there are two kinds of systems which must be considered. The first is a nonautonomous system. This is a driven system, a system that will not oscillate unless there is some external periodic driving force, for example, the driven Duffing oscillator described by the equation

$$\ddot{x}+\gamma x+\beta x^3=A+B\cos(t)\ . \tag{1}$$

For this example and other nonautonomous systems the existence of amplification just before a period-doubling bifurcation has been demonstrated.[13,14]

The other type of system, an autonomous system, is a system which oscillates of its own accord, as does our experimental system. The principal difference between the two systems is that in the nonautonomous system an applied additive external signal is completely equivalent to the driving force, except perhaps for its weaker amplitude. In the case of an autonomous system the external signal is unrelated to the basic oscillation. Experiments showing the existence of amplification before a Hopf bifurcation in such a system have been done by Martin and Martienssen.[15] In this paper we present all the amplification phenomena that we observed in our autonomous delay differential system. This includes, most importantly, amplification around Hopf bifurcations with effects due to higher-order modes, and effects around period-doubling bifurcations. We also study effects of amplification when far from an instability and in a chaotic state. In a final section we discuss the effects of two time delays that can be studied using these amplification phenomena.

THEORETICAL PREDICTIONS

Theories explaining and predicting the various phenomena have been developed by Wiesenfeld and McNamara[10] and by Hackenbracht and Hock.[16] In this section we will present a brief overview of the results of Wiesenfeld and McNamara necessary for understanding the results of our experiments. They consider the first-order differential equation without delay

$$\dot{x}=F(x,\mu)\ , \tag{2}$$

where F is some vector function which may or may not be some periodic function of time, but is a function of some control parameter μ. The influence on the behavior turns out to be relatively independent of the type of modulation, either additive or multiplicative. This is demonstrated by their Floquet analysis. They show that the solution of (2) has the form

$$\phi_k(t)=\sum_k \exp[\rho_k t]P_k(t)\ , \tag{3}$$

where $P_k(t)$ is the set of basis solutions of the unperturbed equation. The Floquet exponents ρ_k determine the bifurcation behavior of the system in one of three ways.

(i) One of the exponents is pure real and crosses the imaginary axis. This gives rise to saddle node, transcritical, and pitchfork bifurcations.

(ii) The imaginary part of one of the exponents crosses the line $\mathrm{Im}\rho=\frac{1}{2}$. This is a period doubling bifurcation.

(iii) A complex conjugate pair of Floquet exponents cross the imaginary axis with an imaginary part different from zero or one-half. This is a Hopf bifurcation, which corresponds to a transition from a steady state to a periodic solution.

Near the bifurcation Weisenfeld and McNamara con-

sider that only one term in the sum is important. It is this term that controls the behavior in the system and gives rise to amplification effects.

For a period-doubling bifurcation the renormalized value of this exponent is

$$\rho_1 = -\alpha + \frac{i}{2} \tag{4}$$

which gives a power spectrum

$$S_m(\omega) = \tfrac{1}{2}\sigma^2 \sum_{j \text{ odd}} \frac{\beta_j \epsilon_k \delta(\omega - \frac{1}{2}j - \Delta) + \delta(\omega - \frac{1}{2}j + \Delta)}{\alpha^2 + \Delta^2} , \tag{5}$$

where the β_j and ϵ_k are constants determined by the form of the perturbation and of the unperturbed solution x_0, and Δ is the distance from the bifurcation.

Thus an external signal near a period-doubling bifurcation produces two peaks of the same amplitude centered around the incipient peak. As a function of frequency the power amplification is predicted to be well approximately by a Lorentzian when a period-doubling bifurcation is approached.

In the case of a Hopf bifurcation, from a fixed point, frequencies which produce large amplification or resonance can be assumed to have the form

$$\Omega = \beta + \Delta , \tag{6}$$

where the important Floquet exponent is

$$\rho_1 = \alpha + i\beta , \tag{7}$$

yielding the power spectrum in the presence of an external frequency Ω

$$S(\omega) = \tfrac{1}{2}\sigma^2 \frac{\delta_0 \epsilon_0^2}{\alpha^2 + \Delta^2} [\delta(\omega - \beta + \Delta) + \delta(\omega + \beta - \Delta)] + \tfrac{1}{4}\sigma^2 \left| \frac{\delta_0' \alpha_0'}{i(\beta + \Delta)} + \frac{\beta_0 \alpha_0}{\alpha + i} \right|^2 \times [\delta(\omega - \beta - \Delta) + \delta(\omega + \beta + \Delta)] . \tag{8}$$

Moreover, the power at the frequency of the applied signal $(\beta + \Delta)$ is a Lorentzian centered around the value of the Floquet exponent.

Although the results of Wiesenfeld *et al.* and Hackenbracht *et al.* are used essentially for ordinary differential equations, they can be applied to problems involving delay differential equations (DDE's), as in our system of the form

$$\dot{y} = f(y(t - \tau_d)) . \tag{9}$$

The solution at a time t of a DDE depends on the solution at every value of time in the interval $(t - \tau_D, t)$. Thus it depends on an infinite number of points and therefore the equation is of infinite dimension. To apply the Floquet analysis it is necessary to decouple Eq. (9) into an infinite system of first-order differential equations with the same form as Eq. (1). This is easily accomplished with the system

$$\begin{bmatrix} y_1 \\ y_2 \\ y_3 \\ \vdots \end{bmatrix} = \begin{bmatrix} f(y_2) \\ f(y_3) \\ f(y_4) \\ \vdots \end{bmatrix} , \tag{10}$$

where $y_1(t)$ is the value of y at t, $y_2(t)$ the value at $t - \tau_D$, y_3 the value at $t - 2\tau_D$, etc. One important result of the infinite dimensionality is that it is possible for a large number of the corresponding Floquet exponents to be on the threshold of satisfying one of the bifurcation conditions. This entails the observation of the predicted effects at more than one frequency.

EXPERIMENTAL SETUP

The experimental setup used for the experiments is illustrated in Fig. 1. The modular consists essentially of an acoustic diffraction grating generated within a piece of flint glass by a radio frequency signal. The laser light enters the crystal at the Bragg angle allowing for the maximum diffraction into the first order which is detected, amplified, and delayed in a magnetic core coaxial cable before being fed back to the modulator. The modification that we made to the basic experimental setup was the addition of an external signal. This was accomplished by adding the differential amplifier of unit gain and injecting the additive external signal at its minus input. The signal was produced by an Hewlett-Packard 8116A signal generator whose output frequency could be externally controlled to a precision of 1 part in 1000. For precise measurements of frequencies and frequency spectra we used a Tektronix 7L5 spectrum analyzer.

The resulting system is modeled by the equation[7,8]

$$\dot{X}(t) + X(t) = \pi\{ A - \mu \sin^2[X(t - \tau_R) - X_B] + \epsilon \sin(\omega t)\} , \tag{11}$$

where A and X_B are bias terms which essentially determine the operating point for the system and ϵ is the coefficient which determines the depth of the modulation of the external signal of frequency. The important parameters are μ and τ_R, the bifurcation parameter being μ

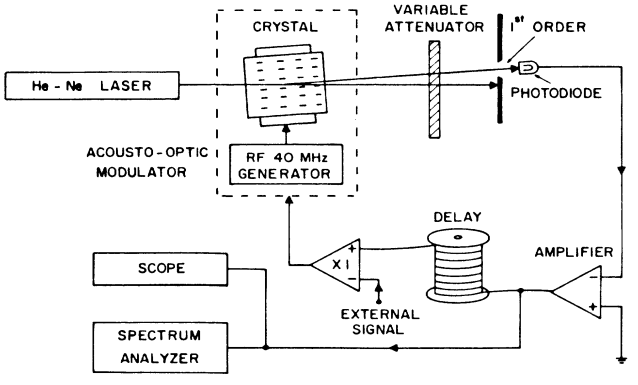

FIG. 1. Experimental apparatus.

and τ_R being the ratio of the total delay time τ_D in the system to its total response time τ.

LINEARIZED-MODE ANALYSIS OF OUR EXPERIMENTAL SYSTEM

The Floquet exponents for our system can not in general be derived analytically. This, however, is not the case before the Hopf bifurcation from a period-1 ($P1$) to a period-2 ($P2$) orbit. In this case the solution has a unique constant value which is easily calculated. Equation (11) can thus be linearized around the fixed point and the Floquet exponents determined. The exponents based on linearization around the fixed point have become known as the linearized modes of the system and can easily be calculated using techniques of linear stability analysis,[17] which are completely equivalent to techniques used in perturbation analysis.

Linearizing the Eq. (11) around its fixed point X^* gives the characteristic equation

$$\gamma\tau+1+\mu\pi\sin[2(X^*-X_B)]\exp(-\gamma\tau_D)=0\ , \qquad (12)$$

where γ is a complex eigenvalue, equivalent to a Floquet exponent. Putting

$$\gamma=\alpha+i\beta \qquad (13)$$

into Eq. (12) and isolating the real and imaginary parts gives

$$1+\tau\alpha+\pi\mu\sin[2(X^*-X_B)']\exp(-\alpha\tau_D)co(\beta\tau_D)=0\ , \qquad (14a)$$

$$\tau\beta-\pi\mu\sin[2(X^*-X_B)]\exp(-\alpha\tau_D)\sin(\beta\tau_D)=0\ , \qquad (14b)$$

which can be solved independently for α and β. The solutions for the γ are then the points of intersection of the two resulting families of curves (Fig. 2). Because of the infinite dimensionality of the system there are an infinite number of solutions, or modes, of these equations. Each of these modes corresponds to a different possible resonant frequency β of the Floquet analysis and thus each should give rise to the same characteristic features predicted by Wiesenfeld and McNamara in the power spectrum.

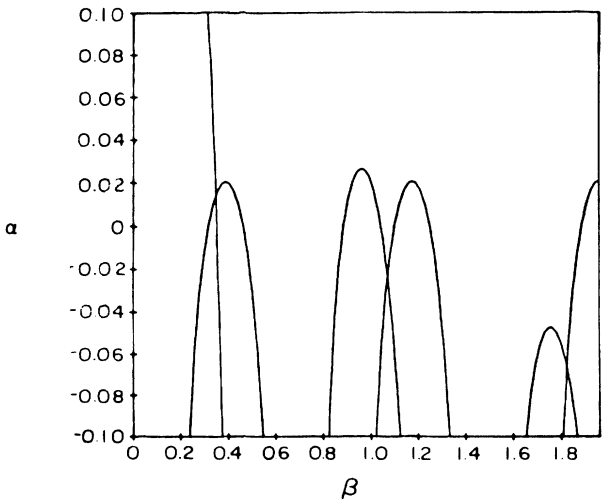

FIG. 2. Solutions of the linearized Eqs. (14). The intersections indicate the solutions for $\tau_R=8$, $\mu=0.45$, $A=0.16$, $X_B=-0.427$.

The importance of the real part of the eigenvalue of Eq. (12) is that it is an indication of the strength of the mode. Normally the first of these modes to traverse the imaginary axis is the one that determines the bifurcation structure of the system. However, the other modes still make themselves visible in our system.

EXPERIMENTAL RESULTS

Experimental procedure

The frequency response of the system at the frequency of the applied signal was measured in one of two ways for various combinations of τ_D/τ, various values of μ, and different values of the external frequency. The response signal was measured either on the oscilloscope for simple wave forms with only one frequency component, or on the spectrum analyzer. The frequency resolution employed with the spectrum analyzer was 100 Hz, as this allowed a reasonable time per sweep and it minimized the possible side effects of averaging frequency over too large an interval as would have been the case with a lower resolution. When using the spectrum analyzer every measurement was made by recording the height of the peak corresponding to the external signal and subtracting the background value measured without the external signal. This was necessary as the level of the background was not always the same due to the effects of noise amplification.

Amplification in the neighborhoods of Hopf bifurcations

Before the first bifurcation we observe perhaps our most significant result, modal amplification. This phenomenon highlights the importance of the linearized modes in the behavior of the system, and also provides a convenient tool for their identification, both experimentally and numerically. It should be mentioned that experimentally they can be put into evidence by noise,[6,7] although not with the same precision as to the form or the location of the mode. In both analytic and computational analysis the use of noise is not elegant and often involves the use of complicated stochastic process theories. The use of a regular signal yields cleaner data that are uncomplicated by the presence of the necessary uncertainties produced by random noise.

Figure 3 shows a typical spectrum produced by the sweeping of the external signal before the first bifurcation. It consists of a background level of 69 mV on top of which are located three regions in which there is amplification of the external signal. At first glance it appears that the regions of amplification are centered around the odd harmonics of the fundamental frequency. This is not the case as was verified by going to the very short delay limit. In this limit the odd harmonics and the linearized modes are not as closely superposed as in the

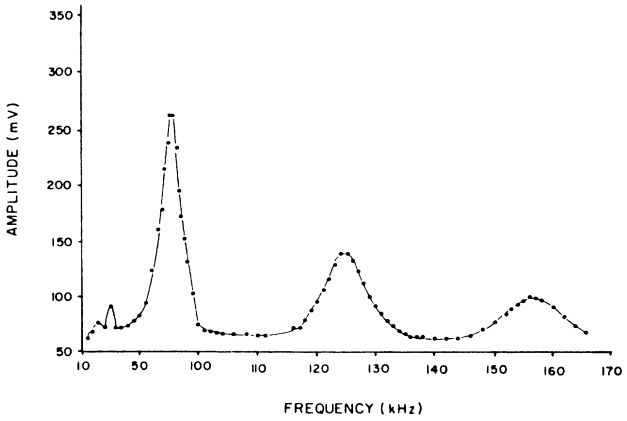

FIG. 3. Experimental amplification spectrum before the first bifurcation. It shows quite clearly the effects of modal amplification. $\tau_R = 8, \mu = 0.45, A = 0.16, X_B = -0.427$.

long delay limit.[17] There are, however, two problems with the short delay limit. The first is that the agreement between the experiment and the numerical model is not as good[18] and the second is that the effect is considerably weaker. This can be explained by the necessity of including higher derivative terms in the model for the short delay limit. These terms affect the linearization and at the same time cannot easily be taken into account by the Floquet analysis. There is also another effect that plays a role. If the system had been a simple ordinary differential equation (ODE) there would only have been a single degree of freedom, implying only one Floquet exponent which in turn implies only one mode. As the delay decreases the effective number of degrees of freedom on the system must decrease, weakening the higher-order mode, until, in the case of zero delay, the number of modes must match the number of modes in the ODE. In our experimental system it has been shown that as the delay is decreased the number of modes ceases to be dependent on the delay but instead becomes dependent on modes due to the effects of higher-order derivatives on Eq. (11).[18] Spectrally, the number of modes that produce observable effects we found was approximately equal to the value of τ_D/τ. This indicates that the effective dimension of the system has approximately the same value. This is in agreement with a recent conjecture of Le Berre *et al.*[19] concerning the dimensions of chaotic attractors in delayed feedback dynamical systems.

Table I lists the frequencies of the maxima of Fig. 2 and their angular frequencies renormalized to units of τ.

TABLE I. Frequency of modes.

Measured frequency (kHz)	Normalized angular (rad)	Calculated angular (rad)	Ratio
75	0.1065π	0.124π	0.95
222	$0.315\,24\pi$	0.338π	0.933
380	0.5396π	0.581π	0.923

These are compared to the calculated values for the modes, and can be seen to be in reasonable agreement. The discrepancies arise from the errors in the measurement of τ_D and τ. Mathematical analysis aside, part of the amplification in the long delay case in the neighborhood of the modes is a result of constructive interference. The period of the frequency of the first mode is well approximated by

$$T = 2(\tau_D + \tau) , \tag{15}$$

where the term $\tau_D + \tau$ can be considered to be the effective delay time of the feedback loop. A signal with a period of $T/2$, if after only one passage through the circuit a signal did not have its sign reversed, or in other words, the signal was not inverted, would be able to interefere constructively with itself after only one passage through the loop. The inversion, however, introduces a phase shift of π which can only be eliminated after a second passage. The period required for constructive interference is thus twice the effective delay time. For higher-order modes the argument is similar.

The form of the regions of amplification around the modes is predicted to be Lorentzian[10] when the amplification is considered a power amplification. Doing least-squares fits to our curves shows, in fact, that the amplitude amplification is the square root of a Lorentzian and therefore that the power amplification is Lorentzian (Fig. 4). The general background level of 69 mV comes from the overlap of the rather long tails of the square root of the Lorentzians.

From the form of the Eq. (8) the half width of these Lorentzians is directly proportional to the value of α or the real part of the eigenvalue λ. Figure 5 shows the value of ϵ calculated from the measured frequency half widths by renormalizing them with respect to τ_R. The agreement is reasonable except when the value of μ is too close to the bifurcation point. The fact that in reality the amplification cannot become infinite, as is required by the Floquet analysis at the bifurcation point, accounts for this. We find that the height of the maxima also depend on α^2, which is illustrated by the best-fit line of slope 2.00 ± 0.03 in Fig. 6. It should be noted that very small values of ϵ are not considered as once again saturation effects must be taken into account which reduce the accuracy of the fit. To take these effects into consideration a nonlinear analysis, including higher-order terms, must be performed.

The fact that the theoretical predictions are confirmed in our system even when sufficiently far from the bifurcation shows that the external signal not only can be used to measure the preferred frequencies of the system, i.e., the imaginary part of the Floquet exponents, but also in a certain fashion the stabilities of these frequencies, i.e., the real parts. If this technique is to be used to measure the values of the exponents, one problem is whether the effect is observable when the value of μ tends towards zero or if, in fact, there is a value of μ at which the effect changes discontinuously. Experimentally, as the value of μ is decreased, the amplification becomes weaker until it reaches the point where it is hidden by the noise. Numerically it is possible to observe the amplification down

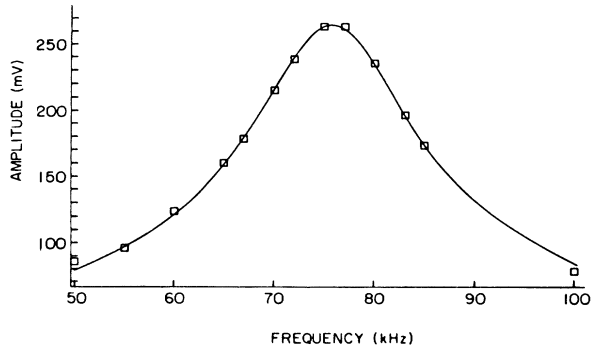

FIG. 4. Least-squares fit of the first peak of Fig. 3 to the square root of a Lorentzian. The best fit obtained was

$$y=\frac{4.60\times 10^{6}\ \text{mV}}{(X-75.73)^2+8.12^2}\ .$$

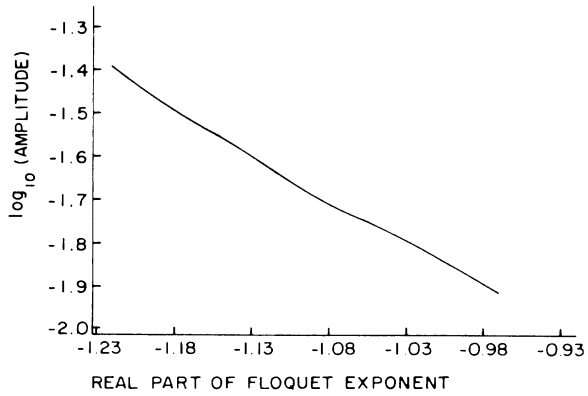

FIG. 6. Log-log plot of square root of maximum power as a function of the Floquet exponent calculated from the half widths. This is done by calculation for $\tau_R=12$, $\mu=0.3$, $\epsilon=0.01$.

to the level of the numerical noise. With decreasing μ the increasing width of the peaks adds a further complication. The positions of the maxima can still be readily measured but their widths and their heights are affected by overlap with the extra width of the neighboring peaks. To determine the values of ϵ these effects would have to be removed (Fig. 7). This is easily accomplished by fitting the resulting curve to a sum of square roots of Lorentzians each centered at the positions of the maxima. Increasing the amplitude of the external signal at small μ does not serve to make the peaks move visible. Its only effect is to multiply the curve everywhere by the same factor.

Amplitudes, however, cannot be increased without limit. The response at some point must cease to follow that predicted by linearized theories. This effect was investigated by studying the output signal amplitude as a function of the input amplitude under various conditions (Fig. 8). As is to be expected with small input signals, the response is linear, gradually increasing until at very large output amplitudes there is saturation. However, when the signal amplitude is very weak, noise starts to play a role, thereby introducing nonlinearities into the response. What is interesting to observe here is that the extent of the linear region is dependent on the input frequency, and that it takes the same form for additive and multiplicative modulations. The response remains linear longest for frequencies that are far from a modal frequency. This demonstrates conclusively that the output cannot be modeled in the same way as the output of a normal amplifying component.

In order to further elucidate the mechanism, the amplification effect was studied to see if the actual presence of the linearized mode was necessary to the amplification, or if, in fact, it was independent. The first mode was thus removed through the use of a selective amplifier (notch or antiresonant filter). It has the effect of attenuating, by more than 100 dB, frequencies within a narrow band centered on some desired frequency. In our case this was the position of the first mode. The width of filtered band depends inversely on the Q factor which was chosen to be as small as possible ($Q=2$) in order to eliminate the largest possible range of frequencies. The results indicate that they are independent. The amplification outside the band filtered by the notch is the same as if it had not been there. In the same manner the

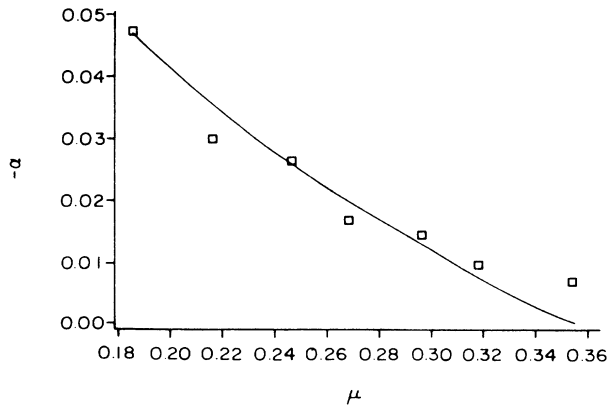

FIG. 5. Value of α, the real part of the Floquet exponent, calculated from experimental half widths and by calculation.

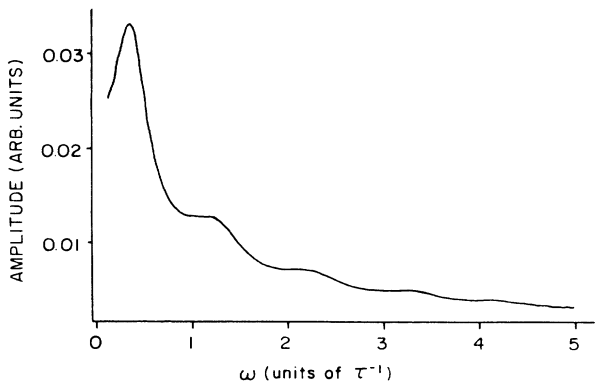

FIG. 7. Observation of amplification effects for very small values of μ. $\mu=0.1$, $\epsilon=0.05$, $\tau_R=8$, $A=0.16$, $X_B=-0.427$.

amplification around the second mode is also unaffected. This implies that, under these conditions, there is no interaction between the modes. It is also to be noted that when narrow filtering windows (high Q) were used the system would adjust its frequency of oscillation so that it would be just outside the window. This change of frequency did not, in any case, change the frequency response of the amplification. It did not recenter itself around the new fundamental frequency, remaining centered around its natural value.

The actual mechanism for the amplification is partially a result of the previously described constructive feedback, but at the same time comes from the dynamics of the underlying mapping:

$$X_{n+1}=\pi[A-\mu\sin^2(X_n-X_B)]\ . \tag{16}$$

Exactly the same phenomena occur for the equivalent discrete map as the bifurcation is approached [Fig. 9(a)]. Geometrically the frequency dependence can be understood from the accompanying figures. For $\omega=2\pi/2$ the condition for a stable orbit leads to the stable orbit shown with the amplification coming from the gradual increase in the slope of the mapping. This increase in slope is nullified for $\omega=2\pi/4$ by the presence of the additional step in the iteration cycle which pulls the two branches of the solution back towards the solution of the mapping without the external periodic signal. This geometric interpretation has been put on an analytical basis by Heldstab.[9]

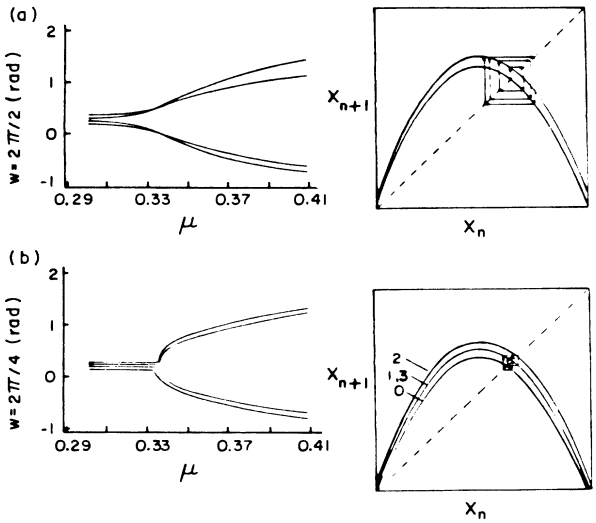

FIG. 9. Amplification effects in the discrete map $X_{n+1}=\pi[A-\mu\sin^2(X_n-X_B)]$ as the first bifurcation is approached. $\epsilon=0.1$, $\omega=\pi$, $A=0.16$, $X_B=-0.427$.

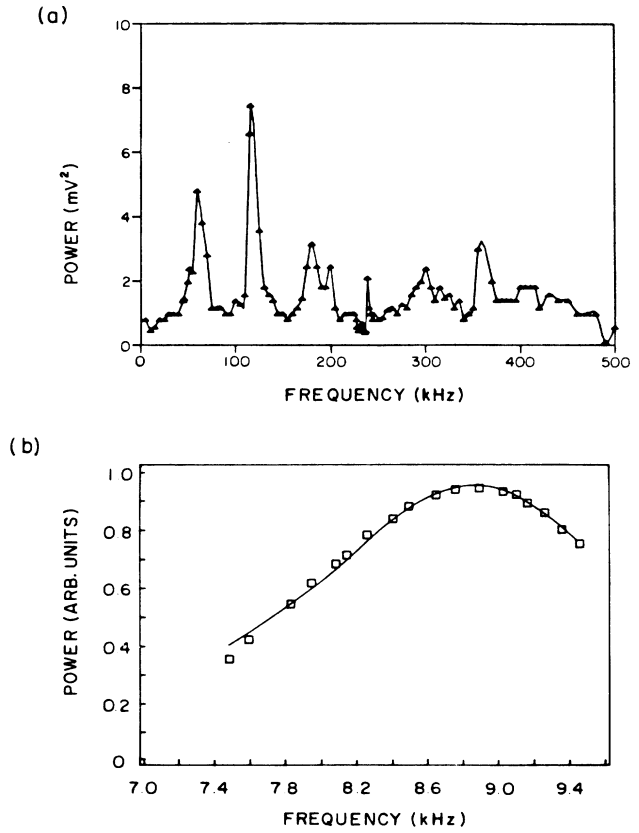

FIG. 8. Variation of output amplitude as a function of input amplitude. In (a) we show the effects of a multiplicative modulation. (b) $\tau_R=8$, $\mu=0.4$, $X_B=0.427$. The frequencies are 40.1, 50.1, and 60.1 kHz, where 60.1 kHz is the frequency of the first mode. The modulation in this case is additive, $\tau_R=8$, $\mu=0.25$, $A=0.16$, $X_B=-0.427$.

In the case of $\omega=2\pi/2$, for the discrete map, and the frequency of the unperturbed $P2$ for the continuous model the system never actually bifurcates from $P1$ to $P2$ as with this choice of frequency the system is always in a period-2 state. In the Lyapunov spectra the normal bifurcation point is marked by the gradual approach of the exponent towards zero and the equally gradual decay away from zero without actually having reached it. This contrasts with the sharp transition present in the case of a normal bifurcation.

How does the amplification actually depend on the variations of the parameters in the system? Figure 10 shows experimental bifurcation diagrams for the system with various external signals. As can be seen from Figs. 9(a) and 10(b) when the frequency is correctly chosen and corresponds to a modal frequency the result resembles the results for the discrete map. With only a very slight deviation from this frequency the result is essentially the same as for the unperturbed case.

To study the amplification effects after the bifurcation, the spectrum analyzer had to be used to measure the response to a frequency that was slightly removed from the frequency of the linearized mode. This had to be done in order to isolate the effects of the external signal from those which were natural to the unperturbed system. The external signal also had to be sufficiently weak so as not to cause entrainment in the system. The measured power response both before and after the bifurcation is illustrated in Fig. 11. As expected, from the results of Weisenfeld *et al.* it reaches a maximum at the bifurcation point. The form of the curve on either side is,

however, somewhat more complicated. Assuming that the values of ϵ vary approximately linearly with μ led us to expect that its form would be reasonably close to a Lorentzian. This is certainly not the case. To correct this manifest lack of fit we tried various μ-dependent weighting functions based on universal scaling properties of bifurcations. As n, the other of the bifurcation, increases, the values of μ_n for each of the succeeding bifurcations get closer and closer together. The desired weighting function was chosen to have the property that this effect would be normalized out and that the effective distance between the bifurcations would be the same. To do this, the idea of a continuum of bifurcations was introduced: between the first ($n=1$) and second bifurcations ($N=2$) there are bifurcations of order $n=1.25$, $n=1.33$, $n=1.47$, etc. For integral n the value of μ at which the

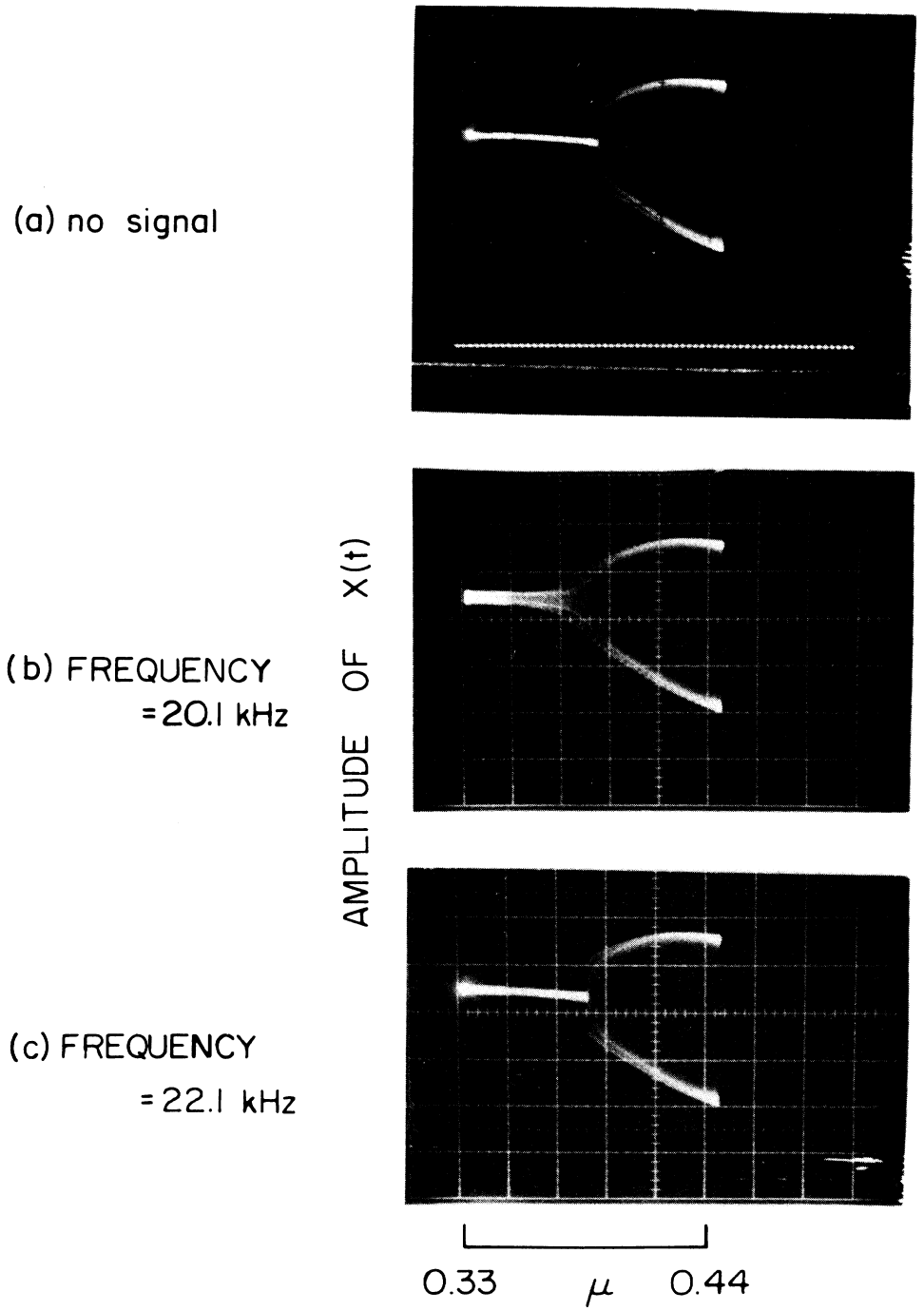

FIG. 10. Bifurcation diagrams showing amplification as the bifurcation is approached. The amplitude of the modulation was 50 mV. $\tau=12$, $A=0.16$, $X_B=-0.427$.

bifurcation occurs is well defined. The problem is to define it for nonintegral n. Feigenbaum's universal result,

$$(\mu_\infty - \mu_n)\alpha\delta^{-n} , \tag{17}$$

where μ_n is the nth period-doubling bifurcation and δ is a universal constant defines it sufficiently. By assuming that the value of n is continuous, it is possible to solve for the corresponding value of the bifurcation parameter μ. But more importantly, it allows for the solution of the weighting function

$$W(u)=\frac{d\mu_n}{dn} , \tag{18}$$

which can be calculated to be

$$W(u)=\frac{[\ln(\mu_\infty - \mu_n)]^2(\mu_\infty - \mu_n)}{C} , \tag{19}$$

where C is a constant to be determined.

This is the weighting function with which we did the fit of Fig. 11. The only additional parameter introduced into the fit beyond the parameters in the Lorentzian was the parameter μ_∞. Its value is not the same as its actual value because the result that was assumed to be an equality is strictly true only in the limit of large n. However, as with the calculation of δ using Eq. (17) the results are still reasonably valid.

RESULTS AFTER THE FIRST BIFURCATION

Beyond the first bifurcation, experiments are complicated by the presence of additional lines in the frequency power spectrum. At these frequencies the system's response to an external signal could not easily be determined. In order to give these frequencies a measured value, their response was assumed to be that of the nearest measurable frequency.

While still far from the second bifurcation the amplification due to the modes continued to play an important role. As the parameter μ increased and the distances from the first bifurcation grew, it approached the position at which the second mode, alone, bifurcates. This resulted in a renormalization of the relative heights of the modal peaks, the second becoming stronger than the first. This occurs because the solution of the first mode moves away from the fixed point solution with the result that the linearized analysis becomes less accurate allowing for a weakening in the strength of the first mode. At the same time the relative magnitudes of the others increased [Fig. 12(a)], as in the chaotic regime where in the immediate neighborhood of an existing peak there is some decrease in the power in the frequency. This was verified both experimentally and numerically and is due to the mechanism previously described [Fig. 12(b)].

Continuing to increase the value of μ brought the system close to the first period-doubling bifurcation. Once again (Fig. 13), amplification was observed at the positions where new spectral peaks would appear after the bifurcation (i.e., $f/2$ and its odd harmonics). The form as a function of frequency is predicted by the Floquet analysis to be a possibly slightly modified Lorentzian. Experimentally, this turns out to be the case [Fig. 13(b)].

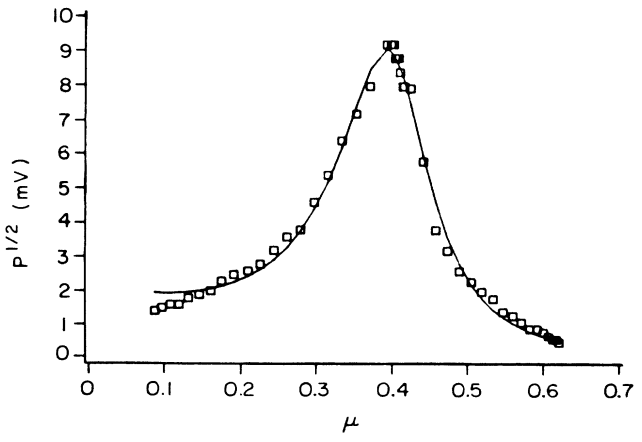

FIG. 11. Growth of amplitude (square root of power P) of response to external signal as a function of μ. $\tau_R=12$, $\epsilon=0.01$, $\omega=2\pi(0.477)/\tau_R$, $A=0.16$, $X_B=-0.427$.

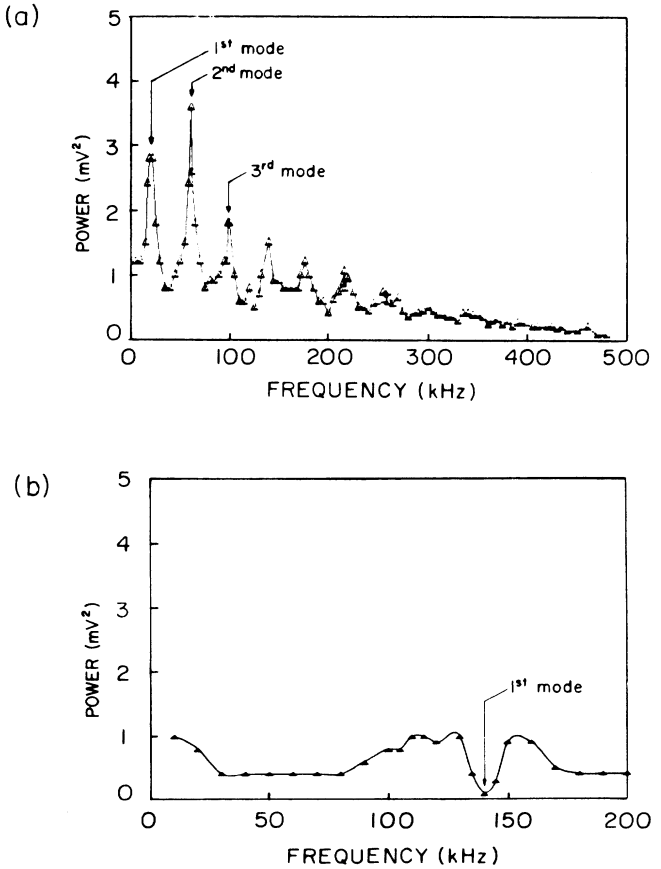

FIG. 12. (a) Modal structure after the first bifurcation. The second mode has become stronger, $\tau_R=12$, $\mu=0.49$, $A=0.16$, $X_B=-0.427$. The modulation amplitude is 100 mV. (b) Deamplification in the neighborhood of a peak present in the system. $\tau_R=2$.

From the parameter values of the illustrated fit the real part of the Floquet exponent governing the bifurcation was calculated to be -2.34×10^{-3}. This is small as is to be expected from the very minor changes produced in the temporal signal at the bifurcation.

The amplification with this bifurcation occurs over a much narrower range of μ than in the case of the first bifurcation (Fig. 14). For higher bifurcations the effects become even narrower, so narrow, in fact, that they become unmeasurable. Nevertheless, the behavior as a function of μ is the same except that it has to be rescaled to the new value of μ and its rate of change with the order of the bifurcation.

After the sequence of period-doubling bifurcations the other type of bifurcation shown by the system is bifurcation from chaos into a periodic window of uneven period. These windows are most easily observed in the short delay limit where several experiments were done just before and just after the transition. In neither case was amplification observed. Amplification is thus not generic to all bifurcations but depends on the bifurcation type. It is not, in fact, to be expected when the system does not change gradually from one attractor to another, as the amplification is a result of the change in form of the attractor. In the case of this transition, there is a sudden jump from a chaotic to a periodic attractor.

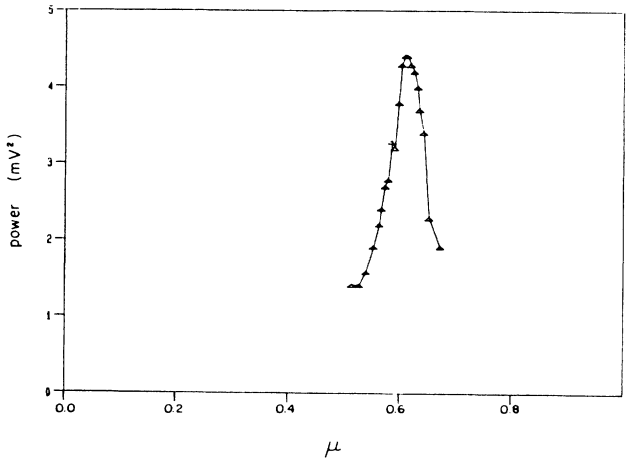

FIG. 14. Amplification around the second bifurcation. The form of the peak is similar to that observed in Weisenfeld's calculations.

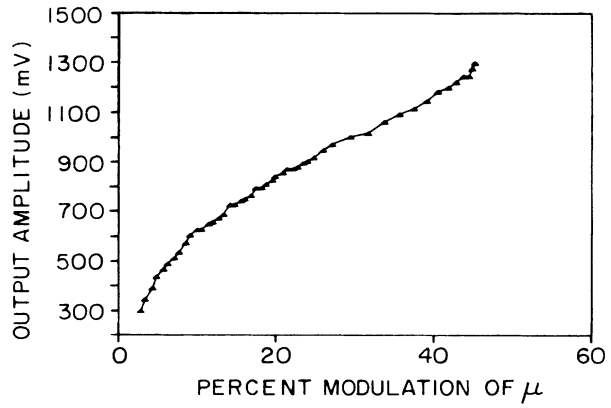

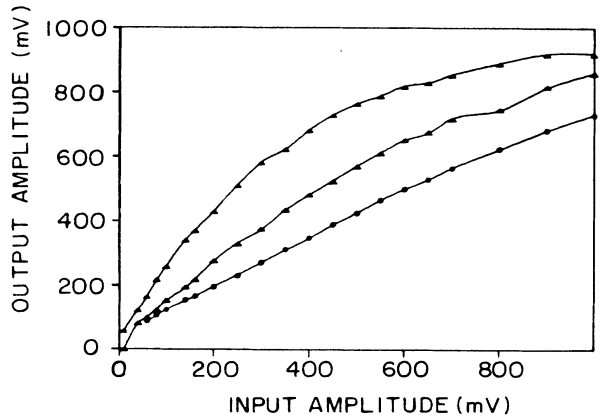

FIG. 13. (a) Amplification just before the second bifurcation. $A=0.16$, $X_B=-0.427$, $\tau_R=4$. (b) A Lorentzian fit to the amplification of the period-doubling bifurcation $\tau_R=13$, $A=0.29$, $X_B=0.367$, $\mu=0.73$. The fit is

$$y=\frac{1.317}{(x-8.85)^2+1.376^2 42}\ ,$$

where $xX^2=0.05$. Top line, 60.1 kHz; middle line, 50.1 kHz; bottom line, 40.1 kHz.

The same applies to the transition from chaos to mode-locked state[20] in which the temporal signal is the result of a combination of signals arising from two modes. Just before the transition no amplification was observed. Thus, there is no change in the underlying dynamics of the system. The transition to a mode-locked state from chaos is therefore just the result of the interaction between the modes concerned.

EFFECTS OF EXTERNAL SIGNAL ON CHAOTIC SYSTEM

In certain situations, especially in fully developed chaos, the system did not strongly react to the external signal. The result was thus the simple incoherent addition of the signals of both the chaotic system and the external generator. This indicates the possibility of further studies concerning the strength of the interaction between the two. However, in developed chaos at very low frequencies (of the order 10^2 Hz), a slight dimunation of the peak height was observed. This can be explained by a distortion of the wave form due to the presence of the chaotic attractor. In this case the dynamics of the chaos play a role. The period of the low-frequency external oscillation is such that in the time required for one oscillation the external signal can make several passes through the feedback loop. This evidently corresponds to several iterations of the related discrete map [Eq. (16)].

With each iteration a little information is lost and the signal looks less and less like a sine wave, with the result that the frequency component at its fundamental is reduced. In the case of higher frequencies one complete cy-

cle can be detected before this phenomena occurs.

When the chaos is not fully developed, i.e., there are still clearly resolved frequency peaks due to the inverse sequence of Lorenz, there are small perturbations to the simple following of the background level. In an interval with a width of the order of 1% of the frequency around the frequency of the remaining peaks the amplitude is slightly increased. In their immediate neighborhood, however, the injected signal and the system's natural frequencies compete, resulting in a reduction of the power in both of the peaks. In the former case, where the signal is not too close to the natural frequency, the slight increase in amplitude can be explained by an entrainment effect. Frequency components that are near to these values diverge less rapidly than more distant signals. The external signal locks in on these components hindering their divergence resulting in a purer signal at these frequencies, which, when added to the external signal, produces a stronger signal at the given frequency. When the frequencies are further away the rate of divergence is too great for any form of locking to take place. The diminuation in the immediate neighborhood is due to the competition between the two frequencies. The cause of this effect can be seen by first considering what happens if the two frequencies are identical. In this case the amplitude of the sum signal is limited by the finite maxima of the transmission function. Therefore, it will not be as great as it would have been had the transmission function been infinite. If the frequencies are slightly displaced exactly the same effect occurs except that the sum must be replaced by the time average of the sum. When the frequencies differ more the effect is less significant.

MODAL EFFECTS OF TWO DELAYS

Modal amplification can be used to study the modal structure of other experimental systems, which can be too complicated for other forms of analysis. Our apparatus with two delayed feedbacks, which can be used to model the Fabry-Pérot system of Ikeda[21] is such a system. Experimentally, because the time delays obtainable were two orders of magnitude too large, we were unable to verify his predictions concerning the sudden jump phenomena which occur when the ratio of the frequencies introduced by the two delays is continuously varied. We were, however, able to observe the interactions between the two delays when they are both of the same order of magnitude.

The circuit used to provide the two feedbacks is illustrated in Fig. 15. The values of τ_D for each feedback loop were adjusted individually and kept constant. Care was taken to ensure that when the two feedbacks were added together the values of A for each loop were halved so that the final value of A, the sum, was equal to the one feedback value.

With only one feedback in the system the linearized modes can be made evident by the amplification of noise in their neighborhoods. Evidently, when there is only one delay in the system we obtain the same modal structure as for the system on which we did the experiments

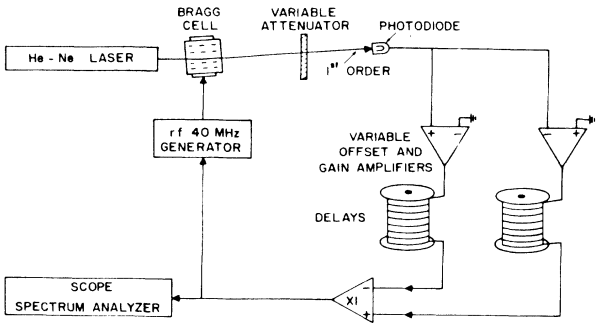

FIG. 15. Experimental setup for the study of the effects of two feedbacks.

with the external signal. In Fig. 16 one can see the effect of the addition of the record delay on the modal structure before the first information. By comparing the three photographs of Fig. 16, it can be seen that the modes remain. The modes of the longer delay are most obvious, but their strengths are modulated by the modes of the shorter delay. Normally, the strength (height) of a mode decreases with increasing order. This is not the case in Fig. 17(c) where the third mode is stronger than all the others. The position of the third mode nearly coincides with the first mode of the shorter delay. This reinforcement of the first few modes occurs at the expense of the second mode of the short delay. With the two delays it cannot be seen, whereas it is quite visible with the short delay alone.

Before the first bifurcation the two delays are independent of one another. After the bifurcation there are three possible scenarios. The first is that both of the delays enter into oscillation independently producing a quasiperiodic state. The second is that one of the delays takes precedence and controls the systems behavior, and the third is that there is a strong coupling between the two with the result that the final frequency is at some frequency other than the natural frequencies of either of the two one delay systems. Figure 17 shows the three possible cases for the temporal signal just after the first bifurcation. From the frequency of the spectra it is evident that the long delay has imposed itself. There has, however, been a slight change in its frequency. Normally, its frequency is 18.4 kHz and that of the short delay is 73.0 kHz. When both delays are present the frequency becomes 19.4 kHz. Thus the effect of the second delay is to slightly increase the frequency. The fact that just after the bifurcation the long delay is the important one can be easily understood by considering the relative strengths of the modes for each delay, those of long delays being in general considerably stronger. From the form of the signals it is easy to see that the added feedback has the effect of smoothing out the square edges of the single delay signal wave. This is to be expected as the second feedback sums the signal with the signal at a time $\tau_1 - \tau_2$ later. The resulting signal is thus similar to an average of the original signal and an exact copy displaced in the time

domain. The bifurcation structure for the three cases is illustrated in Fig. 18. The second delay has had the effect of considerably postponing the bifurcations. Thus the two delays compete, each preventing the other from entering into oscillation until one, the longer, is sufficiently strong. With the two delays a period-doubling bifurcation from $P2$ to $P4$ was never observed.

With this postponement the entrance into chaos is also delayed. Thus when the single delay systems are chaotic the double delay system can be periodic. This periodic state is dependent on the path used to reach it. If reached by gradually increasing μ with both delays in the

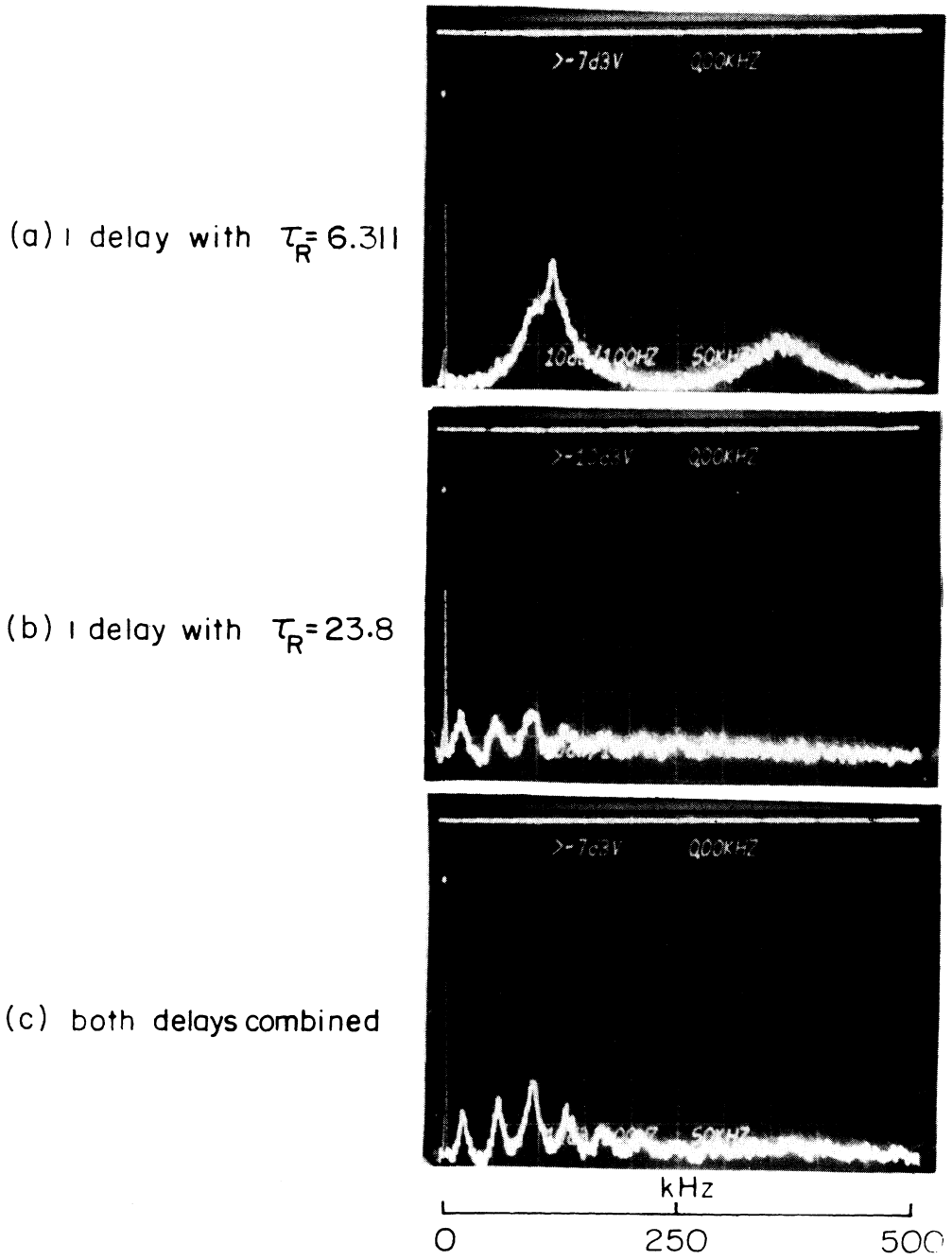

FIG. 16. Modal structure in the presence of two delays. $A=0.16$, $X_B=-0.427$, just before the first bifurcation.

circuit, the same state is reached as when the value of μ is fixed, with only the long delay in the circuit followed by the introduction of the second delay. A different periodic state at the natural frequency of the short delay, however, is attained when the long delay is introduced after the short delay. This hysteresis phenomenon indicates that there are two independent attractors in the system each of which can control the system's behavior.

CONCLUSIONS

In our experiments we have demonstrated the validity of the predictions of Wiesenfeld and McNamara for the

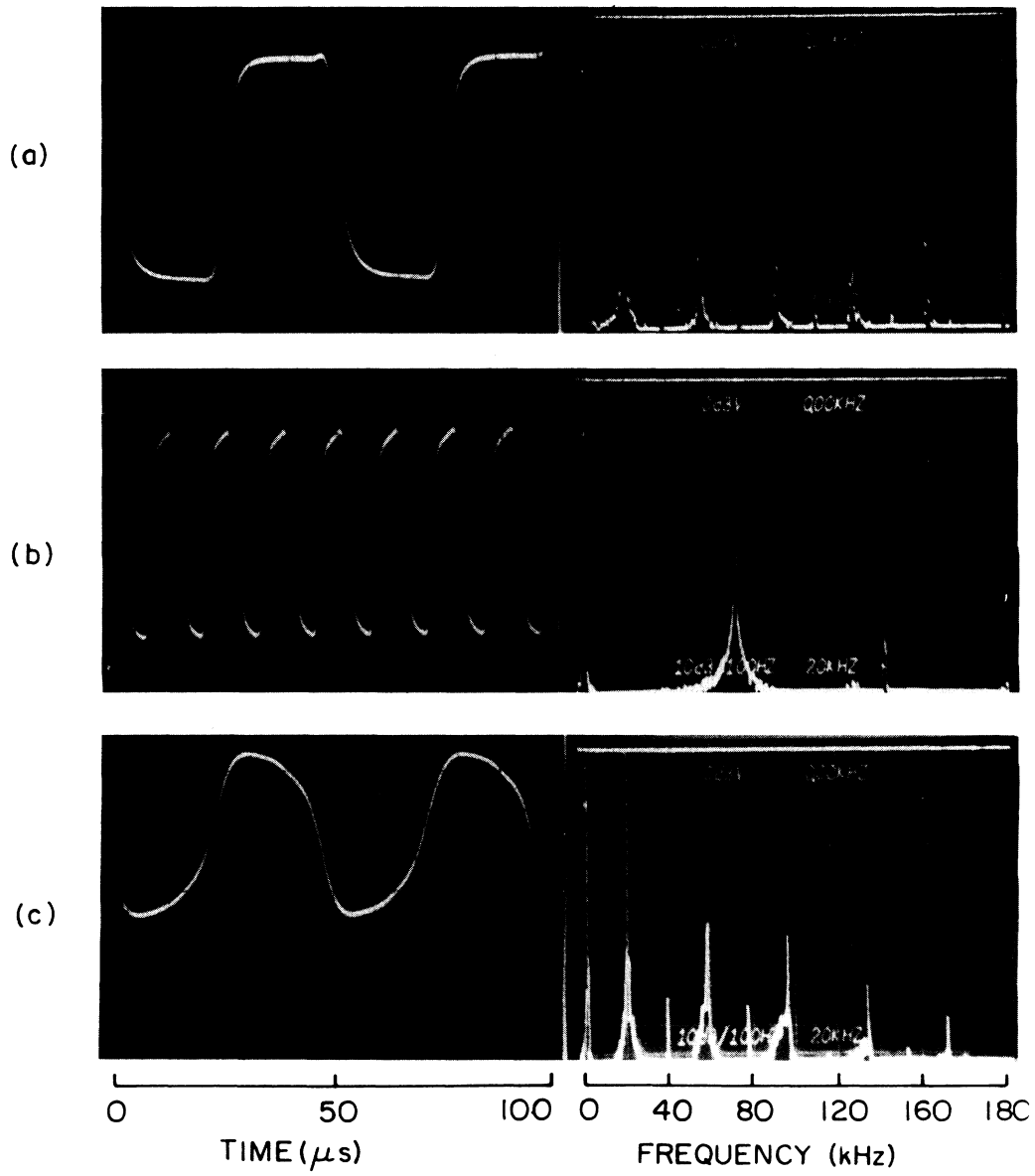

FIG. 17. Effects on the form and spectra of the $P2$ solution in the presence of two delays. (a) $\tau_R = 23.8$, (b) $\tau_R = 63.11$, (c) combined effect. $A = 0.16$, $X_B = -0.427$, $\mu = 0.48$.

Hopf and period-doubling bifurcations of an autonomous system. More importantly, because our system is a delay differential equation, there are an infinite number of degrees of freedom which give rise to effects at other frequencies than those at which spectral peaks appear after the bifurcation. These additional effects can be explained by the linearized modes of the system. We also demonstrated that the modal structure before attaining chaos is independent of interactions between modes. Additionally, we examined the effects when the system was not near a dynamic instability and found regions of deamplification, and regions of amplification when the

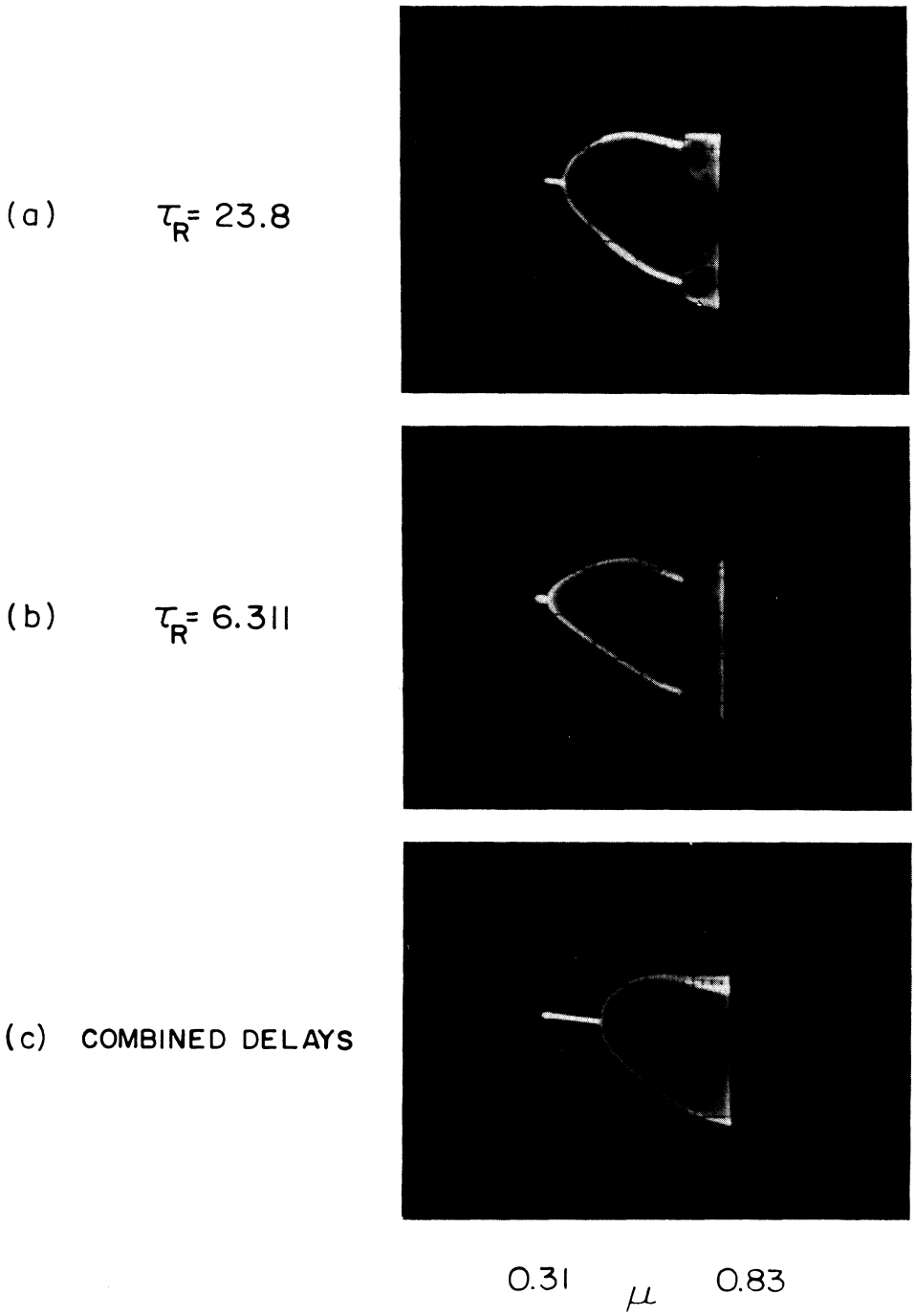

FIG. 18. Suppression of second bifurcation by interaction of two delays. $A=0.16$, $X_B=-0.427$.

system was in a chaos of low dimension. Finally, we used the idea of modal amplification to study the phenomena produced in our system by two delays. We found that the two delays produced slight changes in the bifurcation structure and that they introduced an additional attractor into the system.

ACKNOWLEDGMENTS

We acknowledge the financial support of the Canadian Natural Science and Engineering Research Council as well as the Québec Government through the FCAR. We also thank Réal Vallée for the help he has given us in the final stages of the preparation of the manuscript.

[1]M. J. Feigenbaum, J. Stat. Phys. **19**, 25 (1979).
[2]M. J. Feigenbaum, Phys. Lett. **74A**, 375 (1979).
[3]M. J. Feigenbaum, Los Alamos Sci. **1**, 1 (1980).
[4]M. J. Feigenbaum, Physica D **7D**, 16 (1983).
[5]M. J. Feigenbaum, J. Stat. Phys. **21**, 669 (1979).
[6]C. Jeffries and K. Wiesenfeld, Phys. Rev. A **31**, 1077 (1985).
[7]R. Vallée and C. Delisle, Phys. Rev. A **34**, 2390 (1985).
[8]R. Vallée and C. Delisle, Phys. Rev. A **30**, 336 (1984).
[9]J. Heldstab, H. Thomas, T. Geisel, and G. Radons, Z. Phys. B **50**, 141 (1983).
[10]K. Wiesenfeld and B. McNamara, Phys. Rev. A **33**, 629 (1986).
[11]D. Hackenbracht and K.-H. Hock, J. Phys. C **19**, 4095 (1986).
[12]M. Lucke and Y. Saito, Phys. Lett. **91A**, 205 (1982).
[13]K. Wiesenfeld and B. McNamara, Phys. Rev. Lett. **55**, 13 (1985).
[14]B. Derighetti M. Ravani, R. Stoop, P. F. Meier, E. Brun, and R. Badii, Phys. Rev. Lett. **55**, 1746 (1985).
[15]S. Martin and W. Martienseen, Phys. Rev. A **34**, 4523 (1986).
[16]T. Erneux, S. M. Baer, and P. Mandel, Phys. Rev. A **35**, 1165 (1987).
[17]R. Vallée, Doctoral thesis, Université Laval, 1986.
[18]R. Vallée, P. Dubois, M. Côte, and C. Delisle, Phys. Rev. A **36**, 1327 (1987).
[19]M. Le Berre, E. Ressayre, A. Tallet, H. M. Gibbs, D. L. Kaplan, and M. H. Rose, Phys. Rev. A **35** (9), 4020 (1987).
[20]R. Vallée and C. Delisle, Phys. Rev. A **34**, 309 (1986).
[21]K. Ikeda, and M. Mizuno, IEEE J. Quantum Electron. **QE-21**, 1429 (1985).

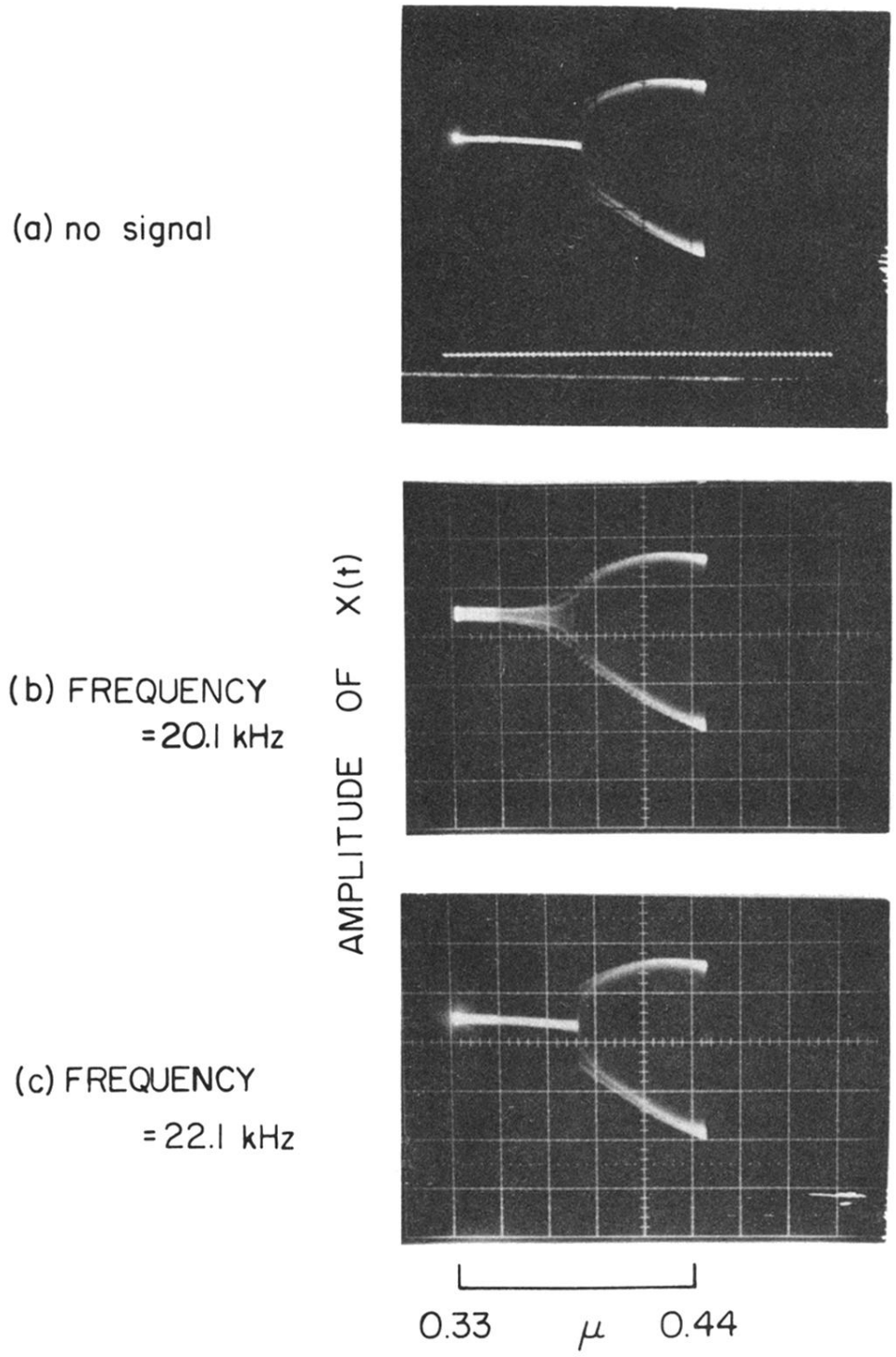

FIG. 10. Bifurcation diagrams showing amplification as the bifurcation is approached. The amplitude of the modulation was 50 mV. $\tau=12$, $A=0.16$, $X_B=-0.427$.

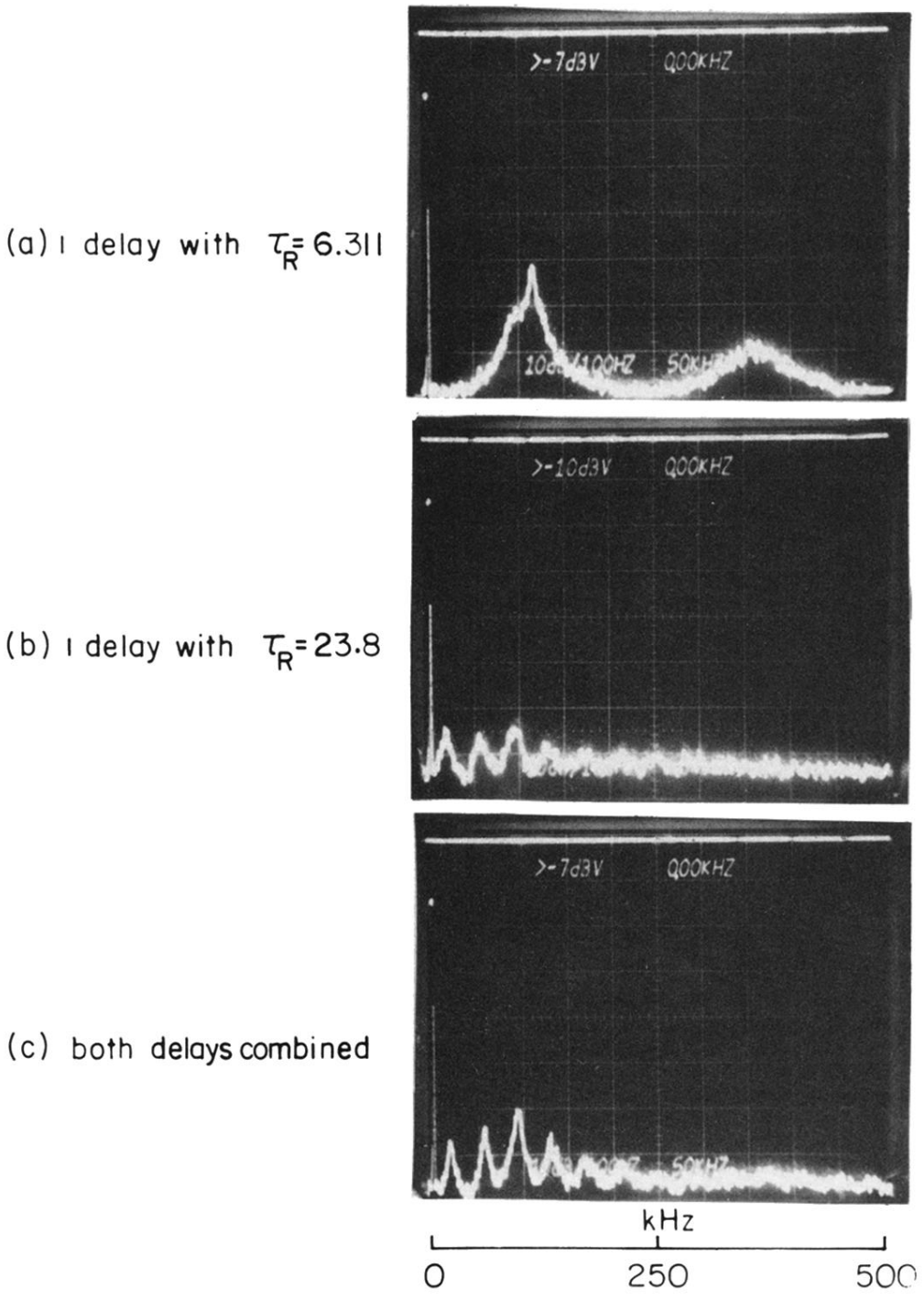

FIG. 16. Modal structure in the presence of two delays. $A = 0.16$, $X_B = -0.427$, just before the first bifurcation.

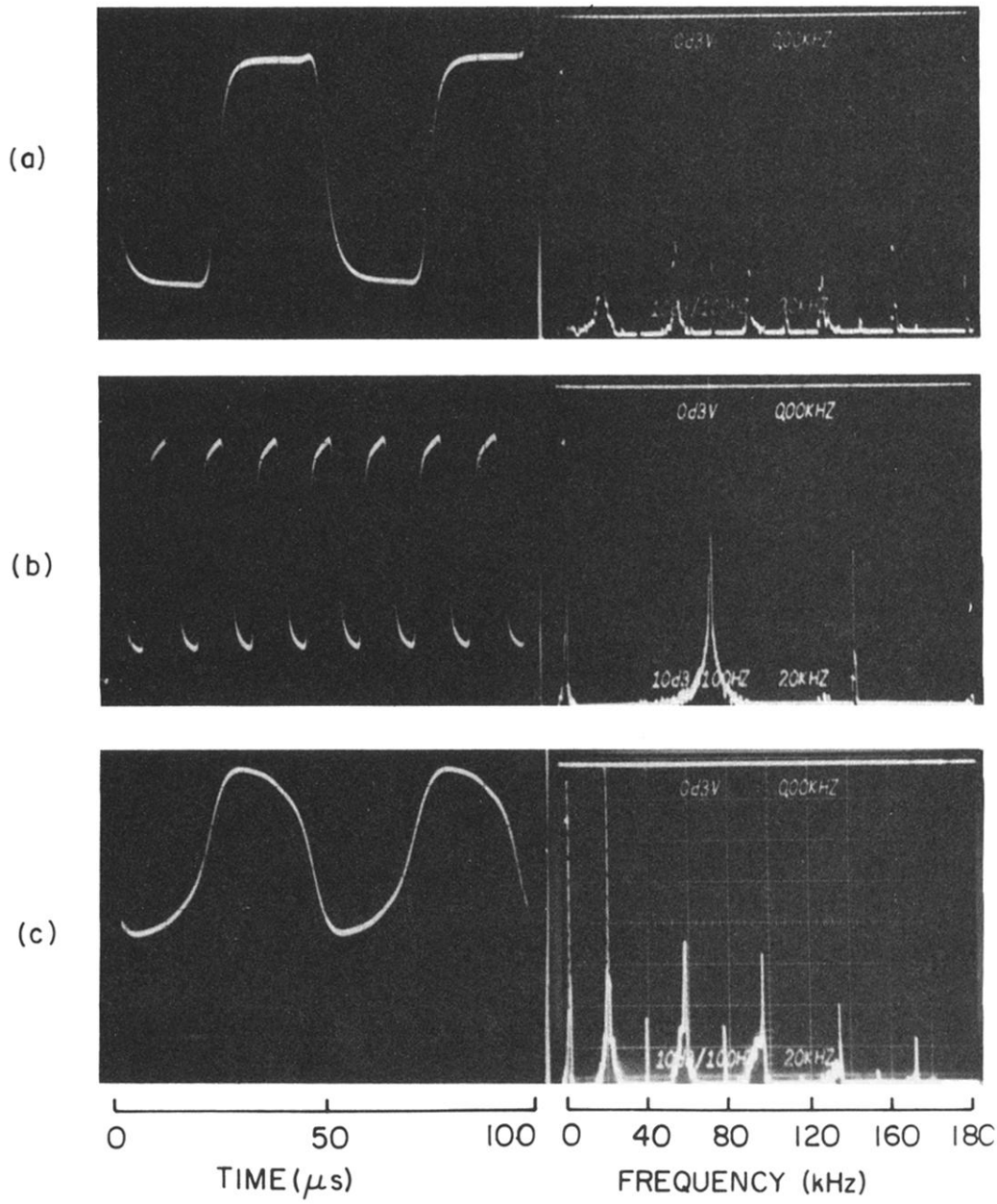

FIG. 17. Effects on the form and spectra of the $P2$ solution in the presence of two delays. (a) $\tau_R = 23.8$, (b) $\tau_R = 63.11$, (c) combined effect. $A = 0.16$, $X_B = -0.427$, $\mu = 0.48$.

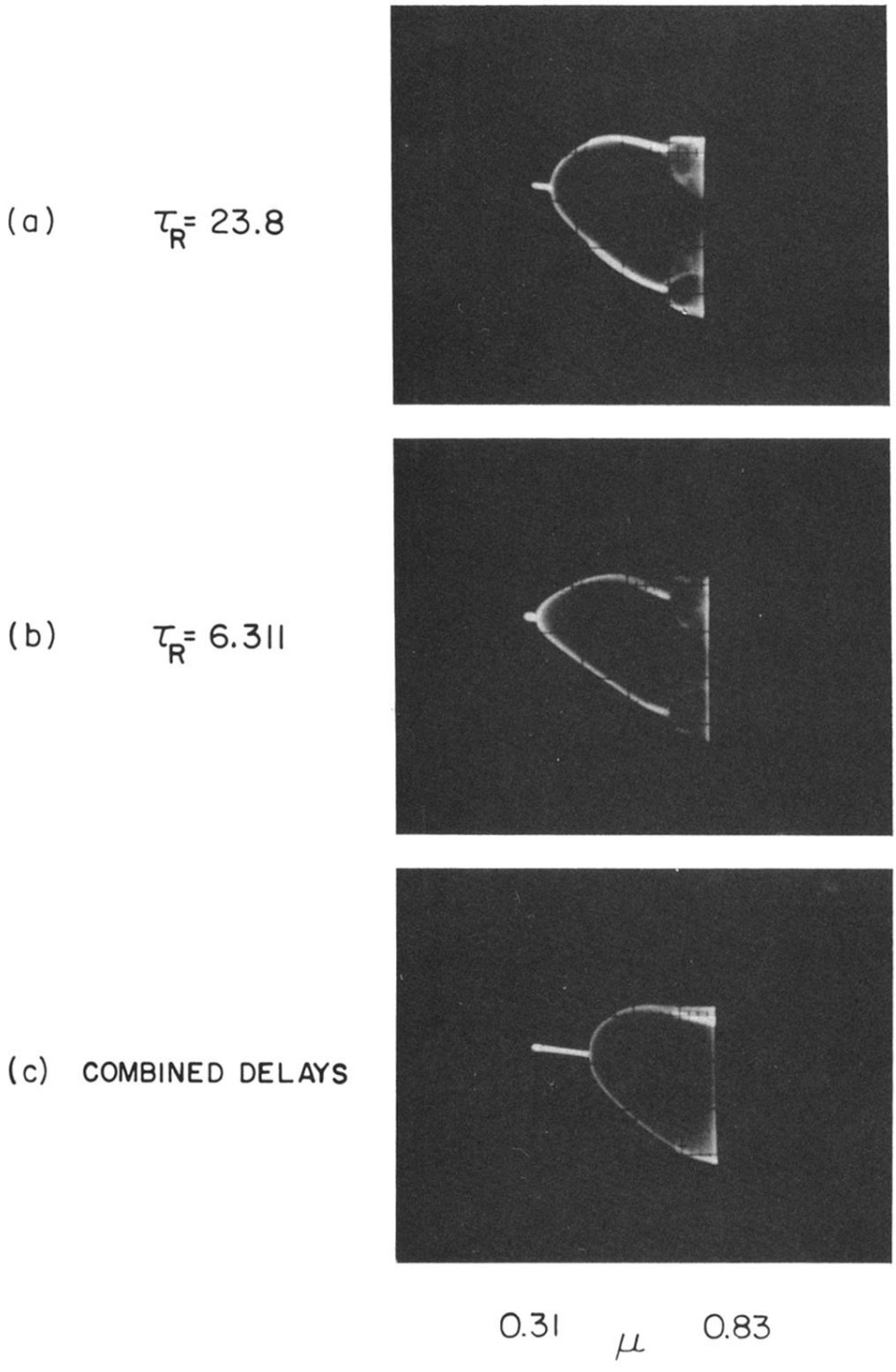

FIG. 18. Suppression of second bifurcation by interaction of two delays. $A=0.16$, $X_B=-0.427$.